Journal of Applied Fluid Mechanics, Vol. 1, No. 1, pp. 78-93, 2008.
Available online at www.jafmonline.net, ISSN 1735-3645.

Mixed Convection in an Enclosure with Different Inlet and Exit Configurations

Sumon Saha[1], Md. Arif Hasan Mamun[2], M. Zakir Hossain[3] and A.K.M. Sadrul Islam[4]

[1]*Lecturer,* [2]*Assistant Professor, Department of Mechanical Engineering,*
Bangladesh University of Engineering and Technology (BUET), Dhaka -1000, Bangladesh
[3]*PhD Candidate, Department of Mechanical and Materials Engineering,*
The University of Western Ontario, London, Ontario, N6A 5B9, Canada.
[4]*Professor, Department of Mechanical & Chemical Engineering,*
Islamic University of Technology, Board Bazar, Gazipur-1704, Bangladesh
Email: [1]*sumonsaha@me.buet.ac.bd,* [2]*arifhasan@me.buet.ac.bd,* [3]*zakir@me.buet.ac.bd,* [4]*sadrul@iut-dhaka.edu*

(Received August 26, 2006; accepted May 27, 2007)

ABSTRACT

A numerical analysis is carried out to study the performance of mixed convection in a rectangular enclosure. Four different placement configurations of the inlet and outlet openings were considered. A constant flux heat source strip is flush-mounted on the vertical surface, modeling an integrated circuit chips affixed to a printed circuit board, and the fluid considered is air. The numerical scheme is based on the finite element method adapted to triangular non-uniform mesh elements by a non-linear parametric solution algorithm. Results are obtained for a range of Richardson number from 0 to 10 at Pr= 0.71 and Re = 100 with constant physical properties. At the outlet of the computational domain a convective boundary condition (CBC) is used. The results indicate that the average Nusselt number and the dimensionless surface temperature on the heat source strongly depend on the positioning of the inlet and outlet. The basic nature of the resulting interaction between the forced external air stream and the buoyancy-driven flow by the heat source is explained by the heat transfer coefficient and the patterns of the streamlines, velocity vectors and isotherms.

Keywords: Finite element, Richardson number, convective boundary, heat flux, electronic cooling

NOMENCLUTURE

C_p	Specific heat of fluid at constant pressure
g	gravitational acceleration
Gr	Grashof number
h	convective heat transfer coefficient
H	height of the cavity
k	thermal conductivity of the fluid
L	width of the cavity
Nu	Nusselt number
p	dimensional pressure
P	dimensionless pressure
Pr	Prandtl number
q	heat flux
Re	Reynolds number
Ri	Richardson number
T	dimensional temperature
u, v	dimensional velocity components
U, V	dimensionless velocity components
$\vec{U}$	velocity vector
w	height of the opening
x, y	Cartesian coordinates
X, Y	dimensionless Cartesian coordinates

Greek symbols

α	thermal diffusivity
β	thermal expansion coefficient
η	kinematic viscosity
θ	dimensionless temperature
μ	dynamic viscosity
ρ	density of the fluid

Subscripts

av	average
H	heated wall
i	inlet state
max	maximum
w	wall

1. INTRODUCTION

Flow and heat transfer due to the combined effect of free and forced (mixed) convection are often encountered in engineering systems, e.g., doubly glazed windows, production of float glass, food processing, growth of crystals, solar ponds, dynamics of lakes and the thermal hydraulics of nuclear reactors. But an important popular field of application of mixed convection is the design of cooling systems for computers and other electronic equipment, where hot sources are usually small and are subject to prescribed heat flux. Careful attention has been taken in designing such systems so that the power requirement for the cooling is minimized to obtain maximum efficiency (Churchill et al, 1976 and Paterson et al. 1990). In an enclosure, the interaction between the external forced stream and the buoyancy driven flow induced by the heat flux from electronic modules leads to the possibility of complex flows. Therefore it is important to understand the heat transfer characteristics of mixed convection in an enclosure.

Various researchers have carried out investigations into the effect of mixed-convective flows in rectangular enclosures by using analytical, experimental, and numerical methods. Angirasa (2000) presented a numerical study of mixed convection of airflow in an enclosure with an isothermal vertical wall. Forced conditions were imposed by providing an inlet and a vent in the enclosure. Both positive and negative temperature potentials were considered by varying the Grashof number of the flow from -10^6 to 10^6. In their study, steady-state solutions could not be obtained for higher positive values of the Grashof number and for buoyancy-dominated flows. In general, forced flows help to enhance heat transfer for both negative and positive Grashof numbers. Hsu and Wang (2000) studied the mixed convection of micropolar fluids (fluids with a non-symmetric stress tensor, their microstructure consisting of rigid, and randomly oriented particles suspended in a viscous medium) in a square cavity with a localized heat source. They indicated that the heat transfer coefficient was lower for a micropolar fluid as compared to a Newtonian fluid. Laminar-mixed convection of a dielectric fluid contained in an enclosure was investigated by Rivas-Cardona et al. (2004). The stability of mixed-convective flows has been analyzed by Leong et al. (2005) for an open cavity heated from the bottom wall. Their analysis concludes that transition to the mixed convection regime depends on the relative magnitude of the Grashof and Reynolds numbers of the flow.

Bhowmik et al. (2005) conducted mixed convection experiments for water simulating electronic chips arranged in-line along a vertical rectangular channel. The experimental results indicated that the heat transfer coefficient was strongly affected by Reynolds number and fully-developed values of the heat transfer coefficient were reached before the first chip. A three-dimensional study of the mixed convection cooling of multiple heat sources flush-mounted on the bottom surface of a horizontal rectangular duct was performed by Wang and Jaluria (2002), Ichimiya and Yamada (2005) and later validation of mixed convection in a differentially heated air cooled cavity was done by several researchers (Moraga and López, 2004, Lo. et al., 2005, and Benzaoui et al., 2005).

More recently, a numerical analysis of laminar mixed convection in an open cavity with a heated wall bounded by a horizontally insulated plate was presented by Manca et al. (2003). Three heating modes were considered: assisting flow, opposing flow, and heating from below. Results for Richardson numbers equal to 0.1 and 100, Re = 100 and 1000, and aspect ratio in the range 0.1–1.5 were reported. It was shown that the maximum temperature values were decreased as the Reynolds and the Richardson numbers increased. The effect of the ratio of channel height to the cavity height was found to play a significant role on streamline and isotherm patterns for different heating configurations. The investigation showed that opposing forced flow configurations had the highest thermal performance in terms of both maximum temperature and average Nusselt number. Later, similar problems for the case of the assisting forced flow configuration were tested experimentally by Manca et al. (2006) and based on the flow visualization results, they pointed out that for Re = 1000 there were two nearly distinct fluid motions: a parallel forced flow in the channel and a recirculation flow inside the cavity. For Re = 100 the effect of a stronger buoyancy force determined the penetration of thermal plume from the heated plate wall into the upper channel.

The effect of exit port locations and the aspect ratio of the heat generating body on the heat transfer characteristics, as well as the entropy generation in a square cavity were investigated by Shuja et al. (2000). They found that the overall normalized Nusselt number as well as irreversibility were strongly affected by both the location of the exit port and the aspect ratio. Omri and Nasrallah (1999) and Singh and Sharif (2003) studied mixed convection in an air-cooled cavity with differentially heated vertical isothermal side walls having inlet and exit ports. Several different placement configurations of the inlet and exit ports were investigated. The best configuration was selected by analyzing the cooling effectiveness of the cavity which suggested that injecting air through the cold wall was more effective in heat removal and placing the inlet near the bottom and exit near the top produced effective cooling.

The present paper applies finite element methods to investigate laminar mixed convection cooling in a rectangular enclosure with a heated vertical wall bounded by adjacent insulated sides. In the present flow configuration, the heated wall placed on the outflow side that provides the highest thermal performance as compared with the other two configurations (Manca et al., 2003). Four different orientations of the inlet and outlet openings are considered, i.e. both the inlet and the outlet openings are placed either on the top or the bottom of the

side walls alternatively. Numerical simulations are carried out over a wide range of Richardson numbers to measure and quantify the best possible inlet and outlet placement configuration to achieve a higher Nusselt number and to obtain minimum temperature inside the enclosure. Also, the temperature and the velocity profiles in the mid-sections of the cavity are presented. The dependence of the thermal and flow fields on the locations of the flow openings is studied in detail.

2. ANALYSIS

The details of the geometry for the configurations considered are shown in Fig. 1. A Cartesian co-ordinate system is used with the origin at the lower left hand corner of the computational domain. The model considered here is an enclosure with a uniform constant-flux heat source q, applied on the right vertical wall. The enclosure dimensions are defined by height H and width L. The other side walls including top and bottom of the enclosure are assumed to be adiabatic. The inflow opening located on the left vertical wall and the outflow opening on the opposite heated wall are arranged as shown in the schematic figures and may vary in location, either top or bottom position. The cavity presented in Fig. 1(a) is subjected to an external flow which enters via the top of the insulated vertical wall and leaves via the top of the opposite heated vertical wall. For reasons of brevity, this case will be referred to as the TT configuration. When the horizontal cold jet enters the enclosure from the top of its insulated wall and leaves from the bottom of the other vertical one, Fig. 1(b), this case will be referred as the TB configuration. Similarly, Fig. 1(c) and 1(d) are referred to as the BB and BT configurations respectively. For simplicity, the heights of the two openings are set equal to one-tenth of the enclosure height. Cold air flows through the inlet at a uniform velocity, u_i. It is assumed that the incoming flow is at the ambient temperature, T_i, and the outgoing flow is assumed to have zero diffusion flux for all variables which are known as convective boundary conditions (CBC) (Sani et al., 1994, and Sohankar et al., 1998). All solid boundaries are assumed to be rigid, with no-slip. The effect of the placement of inlet and outlet on the thermal performance is taken into special consideration

2.1 Governing Equations

The equations governing the conservation of mass, momentum, and energy are used. The flow is considered to be steady, laminar and two-dimensional. Constant thermal properties are assumed except for the density in the body force term of the momentum equation which is modeled by the Boussinesq approximation. Neglecting the viscous dissipation term in the energy equation, the non-dimensional forms of the governing equations in a two dimensional Cartesian coordinate frame of reference can be written as follows,

Continuity equation:

$$\nabla \cdot \vec{U} = 0 \tag{1}$$

Momentum equation:

$$\left(\vec{U}\cdot\nabla\right)\vec{U} = -\nabla P + \frac{1}{Re}\nabla^2\vec{U} - \frac{Gr}{Re^2}\theta\vec{g} \tag{2}$$

Energy equation:

$$\left(\vec{U}\cdot\nabla\right)\theta = \frac{1}{RePr}\nabla^2\theta \tag{3}$$

where $Gr = \dfrac{g\beta q H^4}{k\eta^2}$ $Re = \dfrac{u_i H}{\eta}$ $Pr = \dfrac{\eta}{\alpha}$ $Ri = \dfrac{Gr}{Re^2}$ (4)

Here, X and Y represent the horizontal and vertical directions respectively, $\vec{g}$ is the unit vector in the direction of gravity. Components of the velocity vector $\vec{U}$ are U and V, and P and θ stands for pressure and temperature respectively. In the above system of equations, all the distances are normalized by H, velocities are normalized by the inlet velocity, u_i, and pressure is normalized by ρu_i^2, where ρ is the density of the fluid. The temperature is normalized by $\theta = (T - T_i) / (qH/k)$. The Richardson number, defined as $Ri = Gr/Re^2$, is a characteristic number for the mixed-convection process that indicates the relative dominance of the natural- and forced-convection effects.

2.2 Boundary Conditions

The boundary conditions for this analysis are:

- At the inlet: $U = 1$; $V = 0$; $\theta = 0$
- At the outlet: Convective boundary condition (CBC)
- At the position of the heat source: the dimensionless heat flux at the source is denoted by: $\dfrac{\partial\theta}{\partial X} = -1$
- For the rest of the adiabatic wall: $\dfrac{\partial\theta}{\partial X} = 0$ and $\dfrac{\partial\theta}{\partial Y} = 0$
- No-slip flow condition at the wall: $U = V = 0$

2.3 Heat Transfer Calculations

The heat transfer within the rectangular enclosure is evaluated in terms of the average Nusselt number at the heated wall as,

$$Nu = \frac{1}{L_H}\int_0^{L_H} Nu(y)dy = \frac{1}{L_H}\int_0^{L_H}\frac{h\cdot y}{k}dy \tag{5}$$

with $h = \dfrac{q}{T(L,y) - T_i}$

where L_H is the length of the heated wall and h is the local convective heat transfer coefficient. An index of cooling effectiveness is the bulk average temperature, defined as $\theta_{av} = \int \theta\, dV / V$ where V is the cavity volume.

3. NUMERICAL ANALYSIS

3.1 Computational Procedure

The governing equations are solved numerically using a finite element technique. A mixed finite element (FE) model is implemented with two types of triangular Lagrange elements: an element with linear velocity and

pressure interpolations for the continuity and momentum equations and an element with a quadratic basis velocity and temperature interpolations for the energy equation. A stationary nonlinear solver is used together with Direct (UMFPACK) linear system solver. The relative tolerance for the error criteria is considered to be 10^{-4}. As the dependent variables vary greatly in magnitude, manual scaling of the dependent variables is used to improve numerical convergence. The manual scaling values are kept constant and selected in such a way that the magnitudes of the scaled degrees of freedom become one. The nonlinear equations are solved iteratively using Broyden's method with an LU-decomposition preconditioner, always starting from a solution for a nearby Richardson number. The numerical simulations are performed by varying the number of elements in order to increase the accuracy and efficiency for the solutions. Nonuniform grids of triangular element are employed with denser grids clustering in regions near the heat sources and the enclosed walls. It may be noted that a similar finite element method has been used to solve fluid flow and heat transfer problems in recent investigations by Lo et al. (2005), Roy and Basak (2005), Asaithambi (2003), and van Schijndel (2003).

3.2 Grid Refinement Check

Computations are carried out in an enclosure of aspect ratio (L/H) 1.5 and with dimensionless length of the heated strip set to be 0.9. Preliminary results are obtained to inspect the field variables grid-independency solutions. All tests are performed at Re = 100 and Ri = 10 for each configuration. Using a triangular mesh for two-dimensional simulations, six meshes are used of which, the coarsest mesh has 15170 nodes and 2064 elements (bilinear triangles for velocity); the finest mesh has 75828 nodal points and 11396 elements. Extensive numerical tests are performed and it is found that 7268 mesh elements provide satisfactory spatial resolution for the base case geometry (Table 1) and the solution obtained is to be independent of the grid size with further refinement. Thus, the two-dimensional meshes were found to be sufficiently accurate.

3.3 Validation of the Code

First, the governing equations are solved for the model of a mixed-convective air-cooled room, in order to compare the results with those obtained by Singh and Sharif (2003) . Figure 2 shows the streamlines and isotherms calculated by Singh and Sharif (2003) and the present study for Re = 100 and Ri = 10. Similar comparisons are shown for the results obtained by Manca et al. (2003). The overall tendency of the present results is almost the same as that of calculated by Manca et al. (2003). Another test for validation of this numerical method is performed by similar model simulation as by Manca et al. (2003) and is shown in Table 2. The computed values agree to within 0.5% with Manca et al. (2003).

4. RESULTS AND DISCUSSION

Two-dimensional mixed convection is studied for a laminar flow in an air-cooled cavity with a Prandtl number of 0.71. The controlling parameter, for the four configurations of the geometry as defined in Fig 1(a), (b), (c) and (d), is the Richardson number, Ri. The Reynolds number, Re, is kept fixed at 100. The range of Richardson number used for the simulations is $0 \le Ri \le 10$ and it is obtained by varying the Grashof number only.

The comparison among different configurations for efficient cooling is done based on the maximum surface temperature of the heated wall, the average bulk fluid temperature in the enclosure and the average Nusselt number at the hot wall. For effective cooling, the average Nusselt number at the hot wall should be higher and both the maximum heated surface temperature and bulk average fluid temperature should be lower. The physical analysis of the mixed-convection flow in the cavity is complex due to the interaction of the forced and natural convection. Intuitive inferences are sometimes contrary to the reality. Nevertheless, the dynamics and thermal fields for all the simulations are closely scrutinized. Four different configurations are investigated for the mixed-convection problem in order to compare the behavior of convective heat transfer for different relative inlet and outlet locations.

It is not possible to include the results for all the configurations at all Ri due to space limitation, but some representative streamlines and isotherms are shown for all the configurations at various Ri in Figs. 3–6. Close examination of these flow patterns and temperature distributions reveals the heat transfer phenomena in the cavity for the corresponding configurations. The summary of the simulation results for all the cases are presented in Figs. 8–9 in the form of an average Nusselt number at the hot wall, and an average bulk fluid temperature in the cavity.

As mentioned earlier, the most desirable configuration is that which results in higher average Nusselt number, and lower bulk average temperature. It is observed that injecting air through the insulated wall always gives higher average Nusselt number than injecting air through the heated wall. This can be verified by the results obtained from previous works (Manca et al., 2003), and is due to the impinging effect of the cold stream on the opposite heated wall.

Singh and Sharif (2003) computed the flow for six different configurations considering an isothermal hot wall at one side and a cold wall at the other. Among these configurations, three of them are similar to the TT, TB and BT configurations. They found that the BT configuration produced more effective cooling. However, according to the present computations, both TT and BT configurations are found to be most effective in cooling the cavity, based on the aforementioned criteria. For this reason, detailed analysis is concentrated on the convection processes for these arrangements. It should be mentioned here that the major extensions, made in the present paper to compare with the work of Singh and Sharif (2003), are the application of the constant heat flux surface instead of the isothermal wall, and the replacement of the cold wall by

the adiabatic wall. Also, a new configuration BB (bottom inlet and bottom exit) has been analyzed in the present problem.

4.1 Flow and Temperature Fields

The combined forced and buoyancy driven flow and temperature fields inside a vertical cavity, with a uniform heat source, flush-mounted with the side wall, for different inlet and outlet configurations are illustrated by means of streamlines, velocity vectors and isotherms in Fig. 3-6, for Richardson numbers of 0, 1, 5 and 10. Figure 3 shows the dynamics and thermal field for the TT configuration (injection at the top of the insulated wall and exit from the top of the heated wall) in terms of streamlines, velocity vectors and isotherm surfaces for different *Ri* values. The streamlines and velocity vectors describe the interaction of forced and natural convection under various convection regimes. At *Re* = 100, for the lower *Ri* values, forced convection dominates the major flow from the inlet to the exit without much penetrating into the cavity. The magnitude of the velocity of the cold forced flow decreases as it moves towards the lower horizontal wall, and as the flow comes in the vicinity of the vertical heated wall, the fluid becomes lighter and moves upward towards the exit. Fluid that reaches the bottom wall travels toward the vertical wall and abruptly turns upward, forming a small clockwise circulating Moffat vortex in the corner. When *Ri* is increased to some value between 1.0 and 5.0 a clockwise vortex forms on the upper horizontal wall which increases in size as the Richardson number is further increased, markedly diverting the flow from entrance to exit. This forms a strong assisted flow for the cold fluid up the right heated boundary, thereby faciliting heat transport out through the exit.

Figure 6 shows streamlines and isotherms for the BT configuration. For $Ri < 1$, forced convection dominates and major flow is diagonal from the inlet to the exit. At higher *Ri* (5 and 10), large recirculation zones are formed above the main fluid stream. There is hardly any distortion in the flow streams until the buoyancy and inertia forces become equally dominant at *Ri* = 1. The interaction between the recirculating zone and incoming air jet gets stronger with increase in *Ri* in similar fashion as in the TT configuration. Thermal field is governed more or less by interaction between incoming cold fluid stream and the circulating vortex. It also depends on where the vortex is created inside the cavity. For $Ri < 1$, the high-temperature region is more concentrated near the hot wall and the temperature distribution is more uniform in the remaining parts of the cavity. On the other hand, large temperature gradients close to the hot wall and stratified temperature distribution in the rest of the cavity are observed for *Ri* = 5. With increased dominance of natural convection at *Ri* = 10, the cold incoming air and the hot vortex start to mix up and carry the heat to the bulk of the cavity. The high-temperature zone grows in size, especially in the upper region of the cavity, as the fluid stream is now flowing close to the hot wall first and then going out in the vicinity of the top wall.

4.2 Velocity and Temperature distribution

The vertical velocity profiles and temperature distribution inside the horizontal mid-section of the enclosure are depicted in Fig. 7 for different *Ri* values. It is clear that with the increase of *Ri* the magnitudes of the vertical velocity components increase near the heated solid walls. In the core of the cavity the velocity remains lower, indicating that the fluid is relatively quiet far from the solid boundaries. Taking a closer look at the inflow near the inlet and along its axis, with increasing *Ri*, it can be concluded from Fig. 7 for the TT and BT configurations, that when the governing parameters are large, the vertical velocity component is increased, attains a maximum value, and tends toward zero at the opposite wall. The increase of the velocity components means that the inflow is accelerated inside. In fact, in addition to the buoyancy effect, the pocket of fluid, trapped in the interior, cuts out a part of the momentum from the main flow when the fluid is forced to turn back. In return, this quantity must be released as an aid to the inflow accelerating the fluid. From the observation of the temperature profiles for different configurations we found a similar pattern for both TT and BT configurations.

4.3 Heat transfer

The maximum surface temperature of the heated wall, the bulk average temperature of the fluid and average Nusselt number at the hot wall are compared in Figs. 8, 9 and 10 respectively, for the four configurations. It can be seen that average Nusselt numbers for configurations TT and BT are always higher than the BB and TB cases for the same sets of parameters, whereas the maximum surface temperatures of the heated wall and the bulk average fluid temperatures are always lower for the TT and TB cases. Paying careful attention to Fig. 10 shows that the average Nusselt number is slightly higher for configuration TT for $Ri \geq 2$. But for $Ri < 2$, slightly higher values of average Nusselt number are obtained for configuration BT. Natural convection plays a major role in heat removal for configuration TT, due to the direct impingement of the cold air jet on the hot wall and a relatively large circulation of mixing fluid inside the cavity. Therefore higher heat transfer rates are obtained at higher *Ri* for configuration TT. Both the maximum surface temperature of the heated wall and the bulk average fluid temperature, on the other hand, are found to be lower when the exit is through the top of the heated wall compared to the case when the exit is made through the bottom. For configuration TT, these temperatures are observed to be lowest for most of the cases.

5. CONCLUSION

A numerical investigation of laminar mixed-convective cooling of a rectangular cavity with a constant heat flux source has been conducted to identify the optimum placement of inlet and exit for the best cooling effectiveness.

A total of four inlet/outlet placement configurations have been considered. The study encompasses a constant value of Reynolds number at 100 and a range of Richardson number from 0 to 10, representing dominating forced convection through mixed convection to dominating natural convection. The average Nusselt numbers at the hot wall have been used to compare the cooling effectiveness among different configurations. Results show that the TT and BT configurations have similar performance and the same exit position whereas the BB and TB arrangements have the same nature but a less effective heat transfer rate. Moreover, the configuration with the exit near the top, and the inlet located either at the top or bottom of the wall, produced more effective cooling. But for obtaining higher average Nusselt number, configuration TT ensures maximum efficiency for $2.0 < Ri < 10$ and configuration BT for $0 < Ri < 2$.

REFERENCES

Angirasa, D. (2000). Mixed convection in a vented enclosure with an isothermal vertical surface. *Fluid Dynamics Research* 26, 219-223.

Asaithambi, A. (2003). Numerical solution of the Falkner-Skan equation using piecewise linear functions, *Applied Mathematical Computations* 81, 607-614.

Benzaoui, A., Nicolas, X., and Xin, S. (2005). Efficient vectorized finite-difference method to solve the incompressible Navier–Stokes equations for 3-D mixed-convection flows in high-aspect-ratio channels, *Numerical Heat Transfer, Part B* 48, 277–302.

Bhowmik, H., Tso, C.P., Tou, K.W., and Tan, F.L. (2005). Convection heat transfer from discrete heat sources in a liquid cooled rectangular channel. *Applied Thermal Engineering* 25, 2532-2542

Churchill, S.W., Patterson, C.V.S., and Chu, H.H.S. (1976). The effect of heater size, location, aspect ratio, and boundary conditions on two-dimensional, laminar, natural convection in a rectangular enclosure. *Journal of Heat Transfer* 98(2), 194-201.

Cha, C.K., and Jaluria, Y. (1984). Recirculating mixed convection flow for energy extraction. *International Journal of Heat and Mass Transfer* 27, 1801-1812.

Hsu, T-H., and Wang, S-G. (2000). Mixed convection of micropolar fluids in a cavity. *International Journal of Heat and Mass Transfer* 43 , 1563-1572.

Ichimiya, K., and Yamada, Y. (2005). Mixed convection in a horizontal square duct with local inner heating, *Heat Transfer—Asian Research* 34 (3), 160-170.

Lo, D. C., Young, D. L., and Lin, Y. C. (2005). Finite-element analysis of 3-d viscous flow and mixed-convection problems by the projection method, *Numerical Heat Transfer, Part A* 48, 339–358.

Leong, J.C., Brown, N.M., and Lai, F.C. (2005). Mixed convection from an open cavity in a horizontal channel. *International Communications in Heat and Mass Transfer* 32, 583-592.

Moraga, Nelson O., and López, Sergio E. (2004). Numerical simulation of three-dimensional mixed convection in an air-cooled cavity. *Numerical Heat transfer, Part A* 45, 811-824.

Manca, O., Nardini, S., Khanafer, K., and Vafai, K. (2003). Effect of heated wall position on mixed convection in a channel with an open cavity, *Numerical Heat Transfer, Part A* 43, 259–282.

Manca, O., Nardini, S., and Vafai, K. (2006). Experimental investigation of mixed convection in a channel with an open cavity, *Experimental Heat Transfer* 19, 53–68.

Omri, A., and Nasrallah, S. Ben. (1999). Control volume finite element numerical simulation of mixed convection in an air-cooled cavity, *Numerical Heat Transfer, Part A* 36, 615-637.

Paterson, G.P., and Ortega, A. (1990). Thermal control of electronic equipments and devices. *Advanced Heat Transfer* 20, 181-314.

Roy, S., and Basak, T. (2005). Finite element analysis of natural convection flows in a square cavity with non-uniformly heated wall(s), *International Journal of Engineering Science* 43, 668-680.

Rivas-Cardona, A., Hernandez-Guerrero, A., Romero-Méndez, R., and Lesso-Arroyo, R. (2004). Liquid-mixed convection in a closed enclosure with highly-intensive heat fluxes. *International Journal of Heat and Mass Transfer* 47, 4089-4099.

Sani, R.L., and Gresho, P.M., (1994). Resume and remarks on the open boundary condition minisymposium. *International Journal of Numerical Methods in Fluids* 18, 983-1008.

Sohankar, A., Norberg, C., and Davidson, L., (1998). Low-Reynolds-number flow around a square cylinder at incidence: study of blockage, onset of vortex shedding and outlet boundary condition. *International Journal of Numerical Methods in Fluids* 26, 39-56.

Shuja, S.Z., Yilbas, B.S., and Iqbal, M.O. (2000). Mixed convection in a square cavity due to heat generating rectangular body: effect of cavity exit port locations, *International Journal of Numerical Methods for Heat and Fluid Flow* 10(8), 824-841.

Singh, S., and Sharif, M. A. R. (2003). Mixed convective cooling of a rectangular cavity with inlet and exit openings on differentially heated side walls, *Numerical Heat Transfer, Part A* 44, 233–253.

van Schijndel, A.W.M. (2003). Modeling and solving building physics problems with FemLab, *Building and Environment* 38, 319-327.

Wang, Q., and Jaluria, Y. (2002). Instability and heat transfer in mixed convection flow in a horizontal duct with discrete heat sources. *Numerical Heat transfer, Part A* 42, 445-463.

Table 1- Comparison of the results for various grid dimensions (Re = 100 and Ri = 10.0)

Nodes (Elements)	Configuration	TT	TB	BB	BT
15170 (2064)	Nu	2.276728	1.318137	1.147027	2.2636
	θ_{av}	0.028416	0.149376	0.194099	0.030789
25297 (3622)	Nu	2.276477	1.327863	1.145033	2.2626
	θ_{av}	0.028493	0.147776	0.194856	0.030958
30627 (4442)	Nu	2.276301	1.327963	1.144864	2.26257
	θ_{av}	0.028512	0.147788	0.194912	0.030964
39753 (5846)	Nu	2.276297	1.327952	1.144863	2.262401
	θ_{av}	0.028514	0.147805	0.194919	0.030972
48996 (7268)	Nu	2.27628	1.327974	1.14486	2.262508
	θ_{av}	0.028515	0.147802	0.19492	0.030971
75828 (11396)	Nu	2.276281	1.327978	1.144841	2.262498
	θ_{av}	0.028516	0.147802	0.194927	0.030971

Table 2- Comparison of results for the validation of the code at

Pr = 0.71, Re = 100, Ri = 0.1, w/H = 0.5, L/H = 2

Opposing flow	Present	Manca et al. (2003)
Nu	1.7657	1.7748
θ_{max}	0.629	0.627

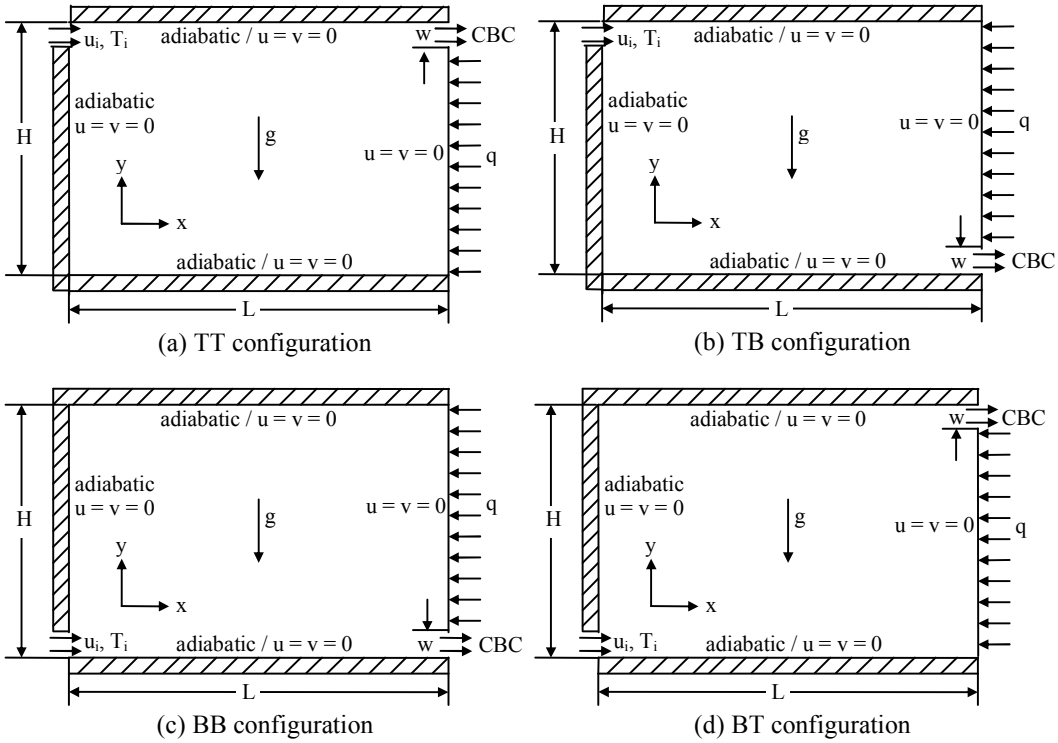

Fig. 1- Four schematic configurations of thermally driven cavity

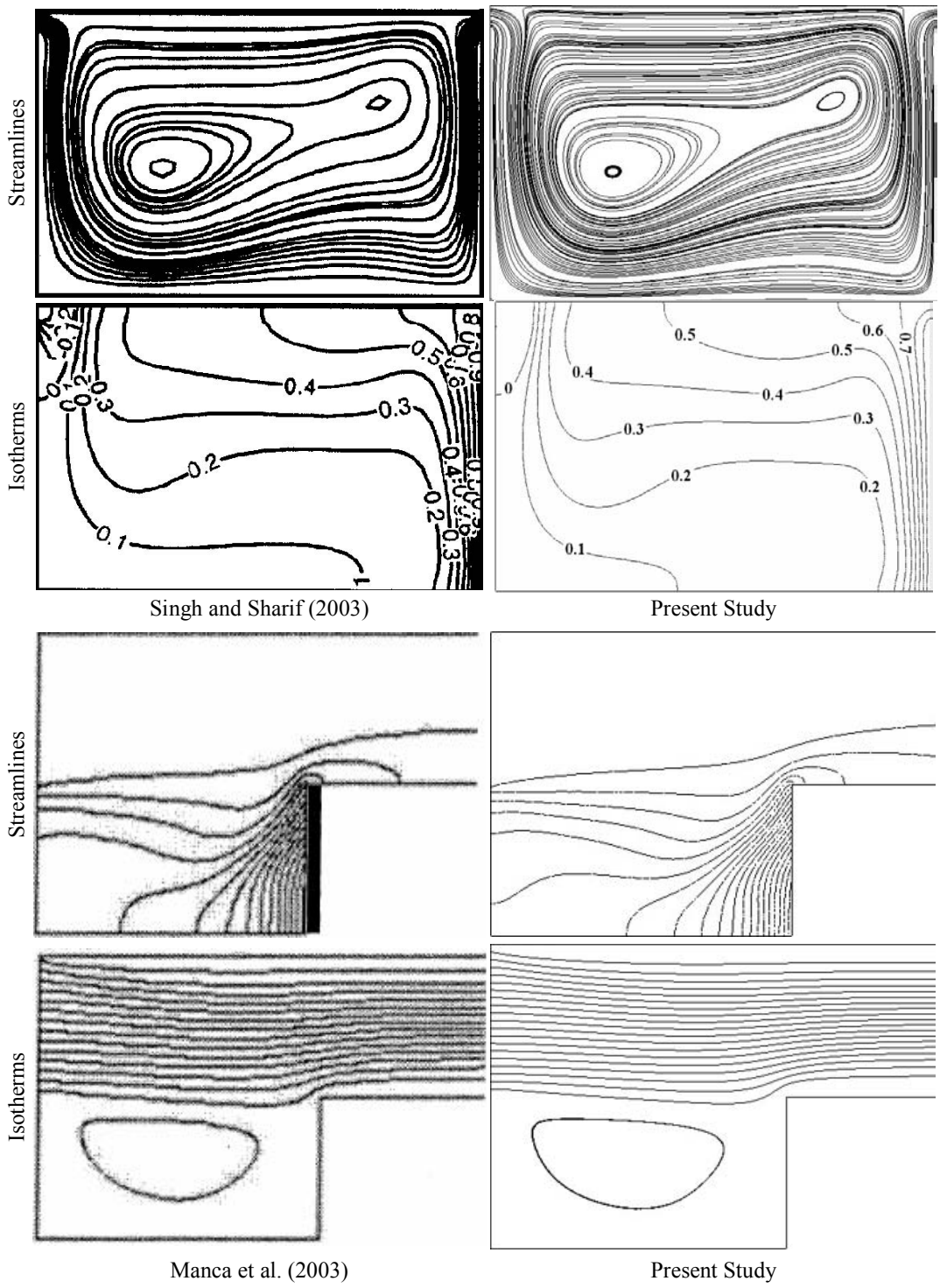

Fig. 2- Comparison of streamlines and Isotherms for results obtained in the present work (right) and those obtained by Singh and Sharif (2003) (upper left) and Manca et al. (2003) (lower left).

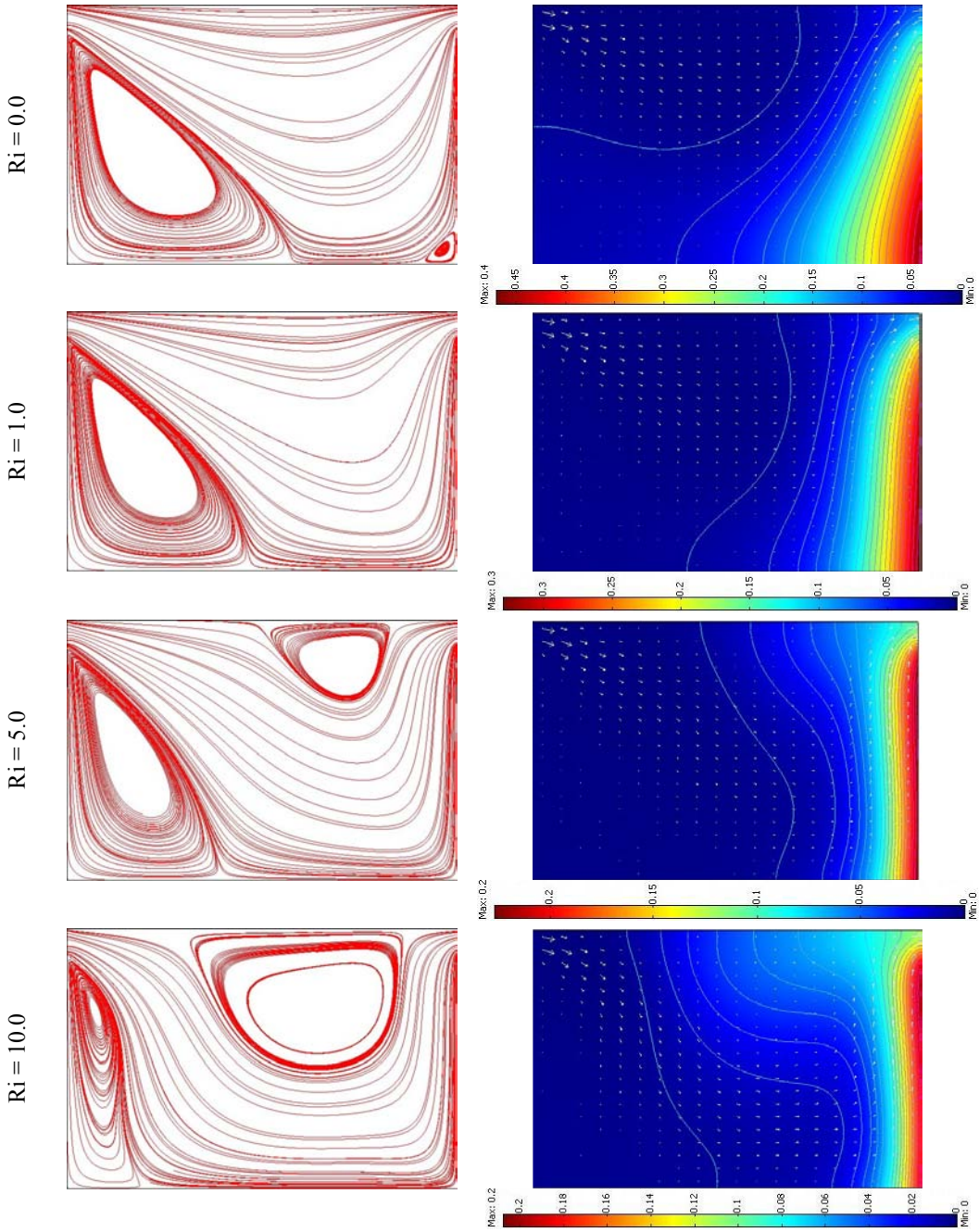

Fig. 3- Variation of streamlines, velocity vectors and isotherms surface for different Richardson numbers for TT configuration

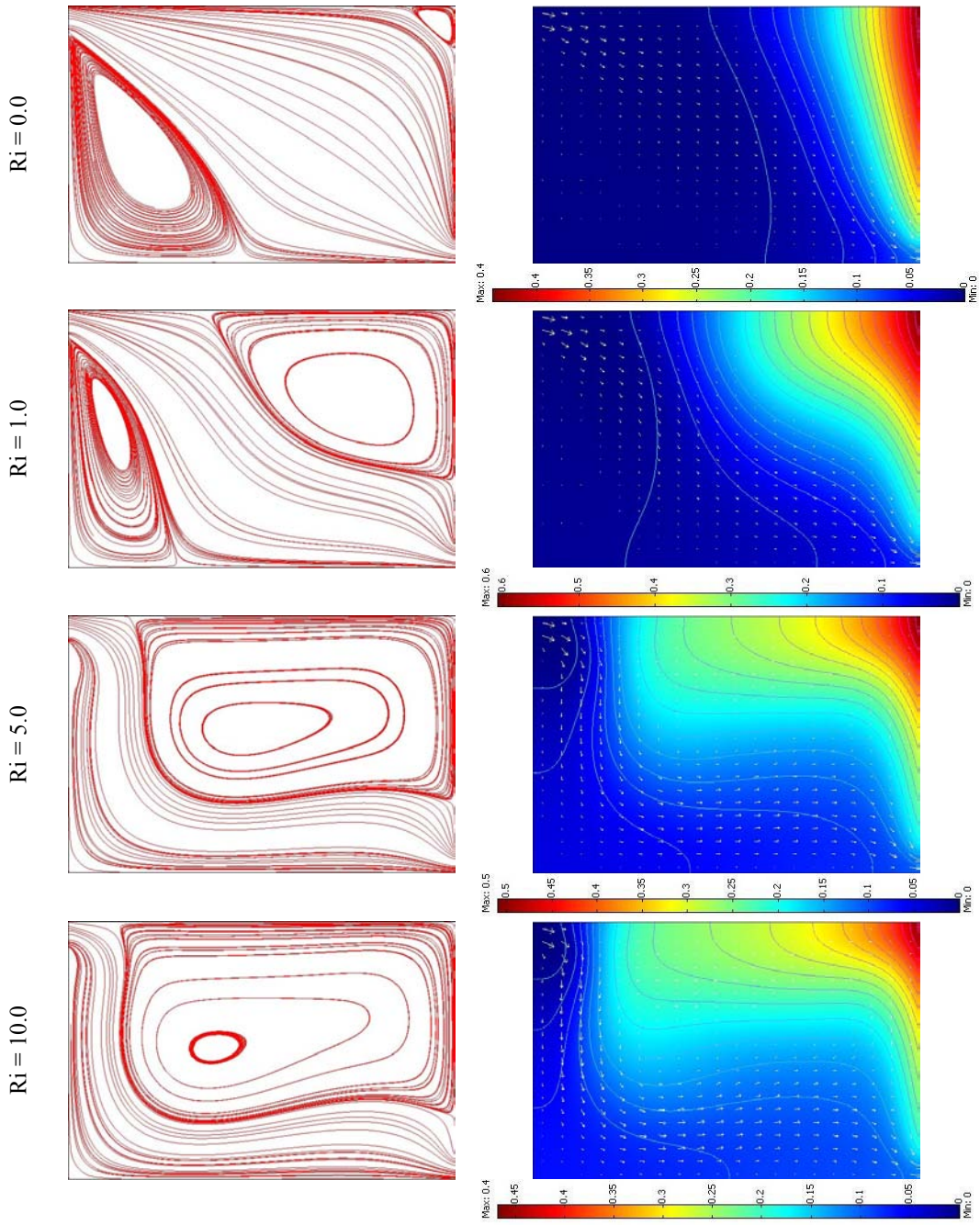

Streamlines Velocity vectors and Isotherms

Fig. 4- Variation of streamlines, velocity vectors and isotherms surface for different Richardson numbers for TB configuration

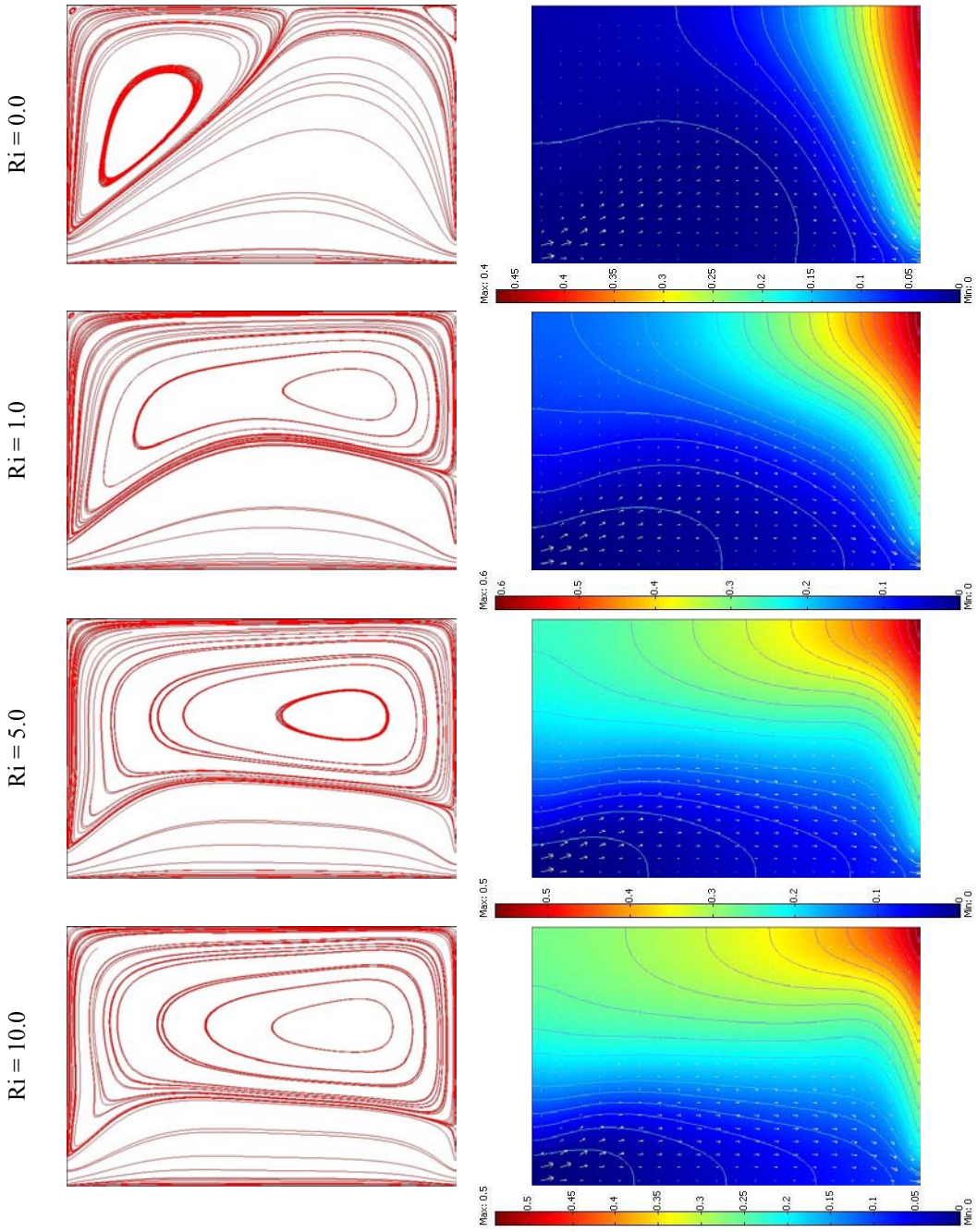

Fig. 5- Variation of streamlines, velocity vectors and isotherms surface for different Richardson numbers for BB configuration

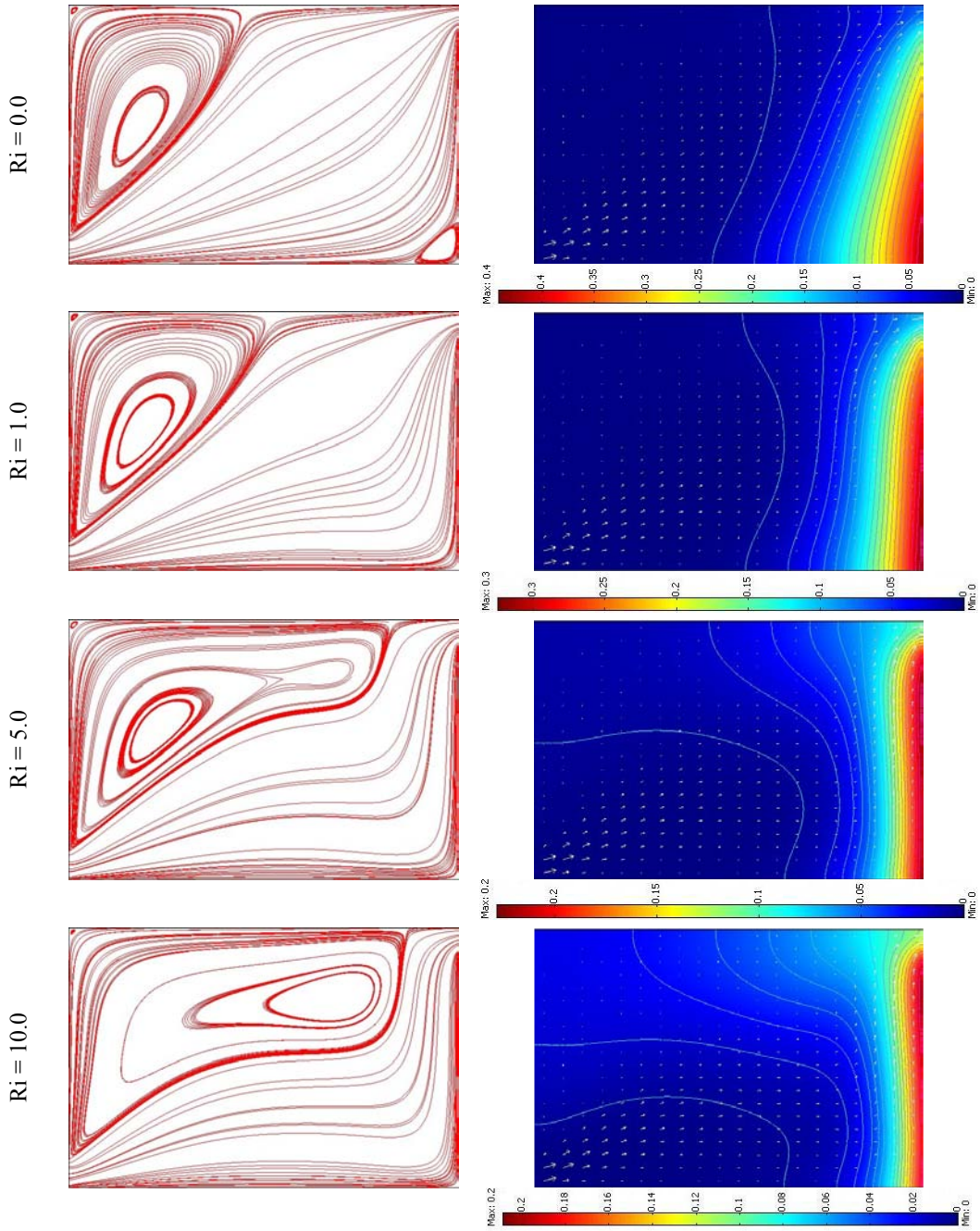

Fig. 6- Variation of streamlines, velocity vectors and isotherms surface for different Richardson numbers for BT configuration

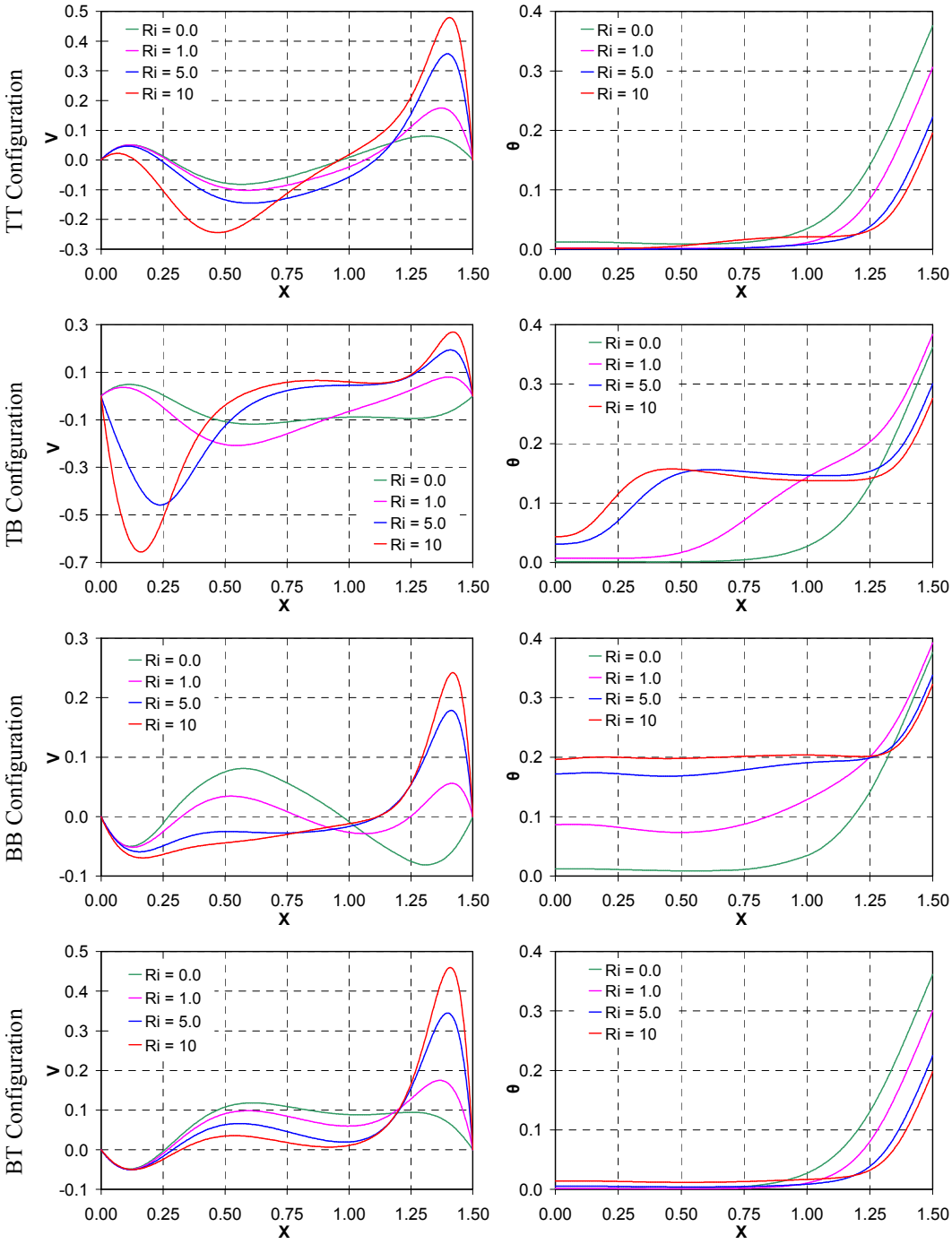

Fig. 7- Effect of Richardson numbers on the vertical velocity and temperature distribution at midsection of the enclosure ($Y = 0.5$) for different configurations

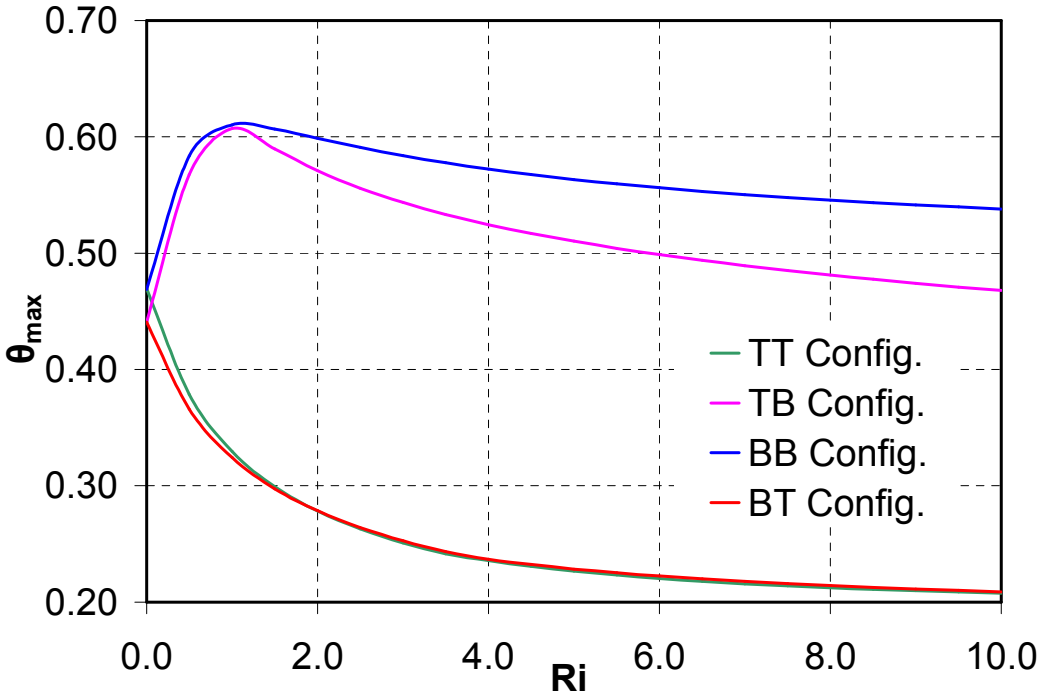

Fig. 8- Comparison of maximum temperature of the heated wall for different configurations

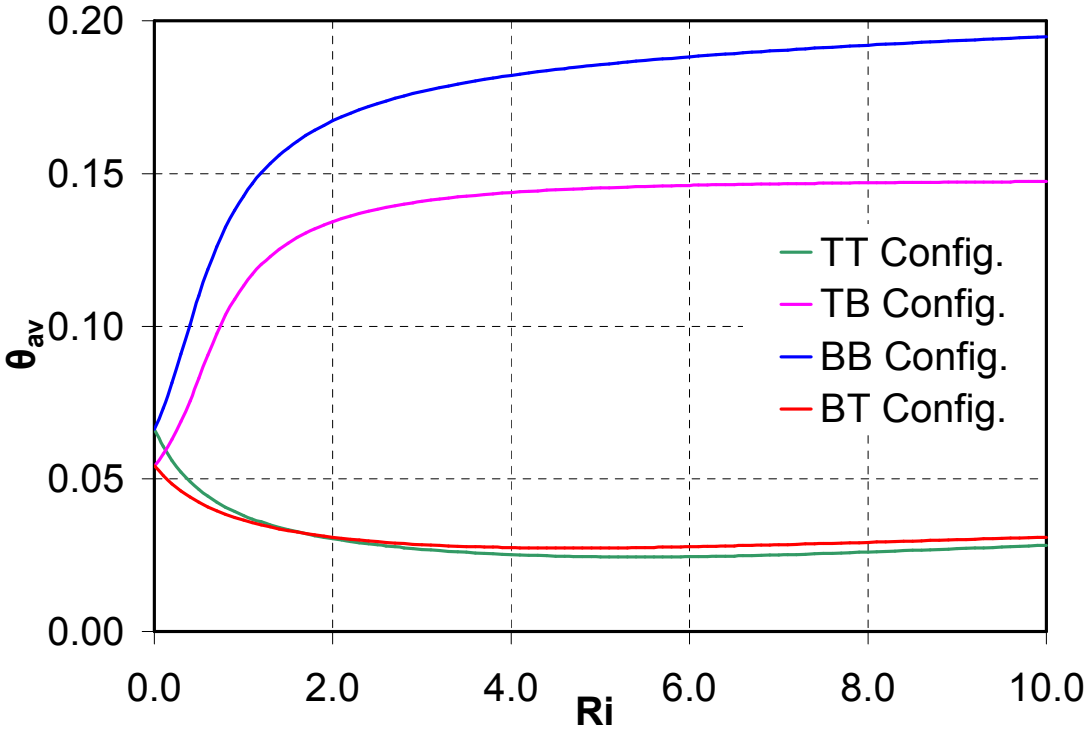

Fig. 9- Comparison of average bulk fluid temperature of the enclosure for different configurations

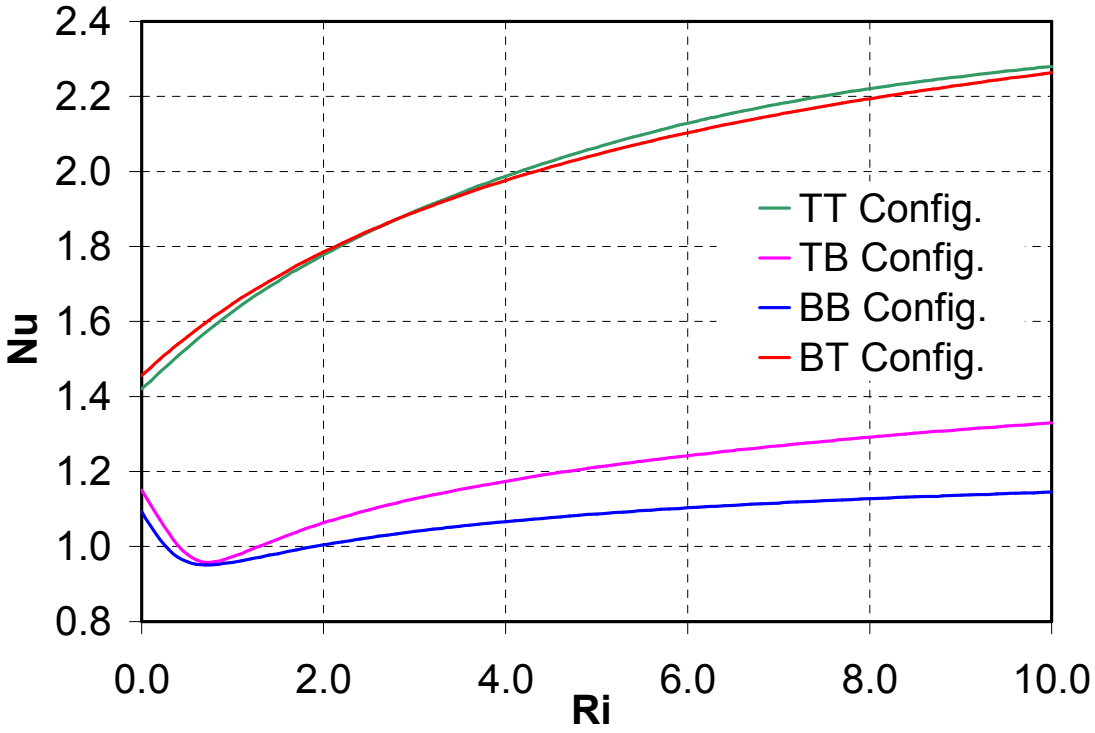

Fig. 10- Comparison of average Nusselt number for different configurations